Complexation of Ln^{III} and Ca^{II} Cations with 3,4-Dicarboxyinulin and Model Compounds: Methyl 3,4-Dicarboxy-α-D-fructofuranoside and 3,4-Dicarboxynystose, As Studied by Multinuclear Magnetic Resonance Spectroscopy and Potentiometry

Louise Johnson,[†] Dorine L. Verraest,[†] Arie C. Besemer,[‡] Herman van Bekkum,[†] and Joop A. Peters*,[†]

Laboratory of Organic Chemistry and Catalysis, Delft University of Technology, Julianalaan 136, 2628 BL Delft, The Netherlands, and TNO Biotechnology and Chemistry Institute, P.O. Box 360, 3700 AJ Zeist, The Netherlands

Received January 31, 1996[⊗]

Complexes of Ln^{III} and Ca^{II} cations with 3,4-dicarboxyinulin (DCI) and model compounds, methyl 3,4-dicarboxy-α-D-fructofuranoside (DCF) and 3,4-dicarboxynystose (DCN) were studied using multinuclear magnetic resonance spectroscopy and potentiometric methods. Complexes of the model compounds with Ln^{III} ions provided a feasible way in which to study complexation phenomena of the dicarboxyinulin/Ca^{II} system using NMR techniques. Information on complex geometry was derived from the effect of Ln^{III} ions on chemical shifts and longitudinal relaxation rates. Metal−ligand stoichiometries of 1:2 and 1:1, in which the ligand coordination was tridentate as well as tetradentate, were found. Potentiometric measurements carried out with Ca^{II} yielded information on the stoichiometry as well as the cooperativity of metal ion binding by the ligands.

Introduction

Inulin (I) is a fructan composed of (2→1)-linked β-D-fructofuranosyl units and a terminal glucopyranoside group. Oxidative cleavage of the vicinal diol units results in a polycarboxylate material, DCI, comprised of a backbone onto which oxidized binding units are attached (Scheme 1). DCI is an excellent Ca-complexing agent, even at a low degree of oxidation,[1] and is therefore considered as a potential candidate for the application as a (co-) builder in detergent formulations.[2] In the soap and detergent industry, there is a continuous demand for new and better products that cost the same or less than the current ones.[3] Insight into the coordination behavior of good Ca(II) sequestering compounds may be helpful for the rational design of future builders and co-builders.

In this paper we present the results of a study carried out on the complexes of DCI and the two model compounds with Ca^{II} and Ln^{III} ions, using multinuclear magnetic resonance spectroscopy and potentiometry.

So far, little is known about the complexation behavior of DCI and the conformation of the Ca^{II} complexes. The complexation phenomena of DCI with Ca^{II} are very complicated due to the intricate polymeric nature of the polycarboxylate. To facilitate studies on complexation characteristics, a model compound, methyl dicarboxy-α-D-fructofuranoside (DCF, Scheme 1) was synthesized in order to represent a dicarboxy inulin unit. Nystose, a tetrasaccharide containing three β-D-fructofuranosyl units terminated by a glucopyranoside group, was similarly converted into a model compound, dicarboxy nystose (DCN, Scheme 1).

Aqueous Ln^{III} and Ca^{II} complexes have often been studied by multinuclear magnetic resonance spectroscopic complexation experiments and potentiometric studies. Ln^{III} ions usually form complexes isostructural with those of Ca^{II} ions, and hence the former can be used as Ca^{II} analogues.[4] Ln^{III} ions in complexes result in significant NMR effects, such as chemical shift changes and relaxation rate enhancements in ^{1}H, ^{13}C, and ^{17}O spectra. The influence of Ln^{III} ions on coordinating ligand nuclei may be obtained from NMR experiments, and these data may then be transformed into information on the structure of the Ln^{III}−ligand complex.[5] Ln^{III} ions interact electrostatically with bound

Scheme 1. Oxidation of Inulin (I), Nystose (N), and Methyl α-D-Fructofuranoside (F)

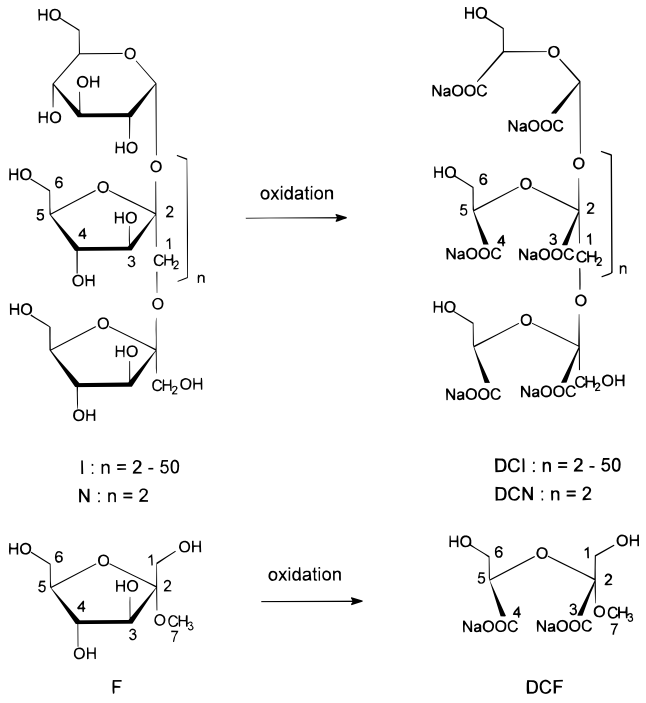

[†] Delft University of Technology.
[‡] TNO Biotechnology and Chemistry Institute.
[⊗] Abstract published in *Advance ACS Abstracts,* August 15, 1996.

(1) (a) Besemer, A. C.; van Bekkum, H. *Recl. Trav. Chim. Pays-Bas* **1994**, *113*, 398. (b) Floor, M.; Schenk, K. M.; Kieboom, A. P. G. *Starch* **1989**, *41*, 303.
(2) Besemer, A. C.; van Bekkum, H. Patent Application WO17189, 1993.
(3) Ainsworth, S. J. *Chem. Eng. News* **1996**, Jan. 22, 32.
(4) Martin, R. B. In *Calcium in Biology*; Spiro, T. G., Ed.; Wiley: New York, 1983; Chapter 6.

S0020-1669(96)00103-6 CCC: $12.00

ligands; thus the coordination geometry of Ln^{III}−ligand compounds reflects a balance between electrostatic, steric, and solvation requirements.[6] Potentiometric studies on Ca^{II} complexation yield information on Ca^{II} complex stoichiometries as well as the cooperativity of binding by the ligand.

Experimental Section

Materials. DCF was synthesized according to a previously reported procedure.[7] Initial experiments involved oxidations using a sodium hypochlorite/bromide system, however oxidation byproducts as well as the formation of large quantities of salt led us to seek an alternative synthetic method. The more successful method involved oxidation first with $NaIO_4$ and then with $NaClO_2/H_2O_2$, and in this way DCF was obtained in good yield as the disodium salt. Nystose was donated by Südzucker and was similarly oxidized to form DCN as the disodium salt. Inulin (ex chicory, average DP = 20) was converted into the dicarboxylate using a two-step oxidation with $NaIO_4$ and then with $NaClO_2$.[8] The oxidation degree obtained was >95%. Formic acid was produced as a side product during the $NaIO_4$ oxidation of nystose and inulin because the C3 atom is eliminated during the glycol cleavage of the glucopyranoside moiety. Thus the DCN and DCI compounds are composed of equivalent oxidized saccharide units. The various Ln^{III} salts were purchased from Sigma in the form $LnCl_3 \cdot 7H_2O$. $CaCl_2 \cdot 2H_2O$ was purchased from Merck.

NMR Measurements. ^{17}O measurements were performed at 27.12 MHz on a Nicolet NT-200 WB NMR spectrometer at 346 K using 16-K datapoints and a spectral width of 20 kHz. The ^{17}O signal of water was shifted by the addition of incremental amounts of $DyCl_3 \cdot 6H_2O$ to a 0.1 M sample of the ligand in D_2O. The measurements for each ligand were accompanied with a calibration experiment (measurement without ligand) at the same temperature. ^{13}C spectra were recorded on a Varian VXR-400 S spectrometer at 50.31 MHz with D_2O as solvent and *tert*-butyl alcohol as internal standard (CH_3: δ = 31.2 ppm). The ^{13}C longitudinal relaxation times were measured using an inversion−recovery pulse sequence with a composite 180° pulse. The ^{13}C longitudinal relaxation times were calculated using a nonlinear three-parameter curve-fitting procedure.[9] Longitudinal diamagnetic ^{13}C relaxation rates were obtained from measurements carried out on the diamagnetic $La(DCF)_2$ complex and free ligand as individual, degassed solutions.

The computer program ALTONA was used to calculate plots of vicinal H−C−C−H dihedral angles from proton−proton NMR vicinal coupling constants. This program employs an empirically generalized Karplus-type equation which takes into account electronegativity as well as the orientation of substituents attached to the vicinal system concerned.[10]

Optical Rotation. The measurements were performed at 25 °C on a Perkin-Elmer 241 polarimeter. Optical rotation values of ligand solutions (12.5 mM), containing increasing amounts of Ca^{II}, were measured.

Calcium Sequestration Experiments. The measurements were carried out using a Unicam IS-Ca Ion selective electrode and a Unicam RE15 double junction reference electrode (Unicam Analytical Systems, Cambridge, U.K.). Calibration was performed in the range 10^{-1}−10^{-6} M. The ionic strength was maintained at 0.02 M using NaCl. A Ca^{II} concentration reading was taken after each addition of an aliquot of $CaCl_2$ solution to a ligand solution (0.1 g in 0.1 L) at pH 10.2 (NH_3). The Ca^{II} sequestering capacity (SC) is defined as the number of millimoles of Ca^{II} bound per gram of ligand.

Viscosity Measurements. Viscosity measurements of Ca^{II}−DCI complexes were performed at room temperature using a Bohlin CS Rheometer and are reported as relative viscosities (Pa s) from which the viscosity of the free ligand has been subtracted.

Results and Discussion

Complications encountered when studying aqueous structures of macromolecular complexes such as $Ca(DCI)_2$ include poor spectral resolution and difficulties due to the complicated phenomenon of multiple binding sites. Hence in this study, simpler ligands, e.g. DCF (one oxidized saccharide unit) and DCN (four oxidized saccharide units), proved to be useful as model molecules of DCI in complexation experiments. For the NMR experiments, Ln^{III} ions, (Dy^{III}, Gd^{III} and La^{III}) were used as model ions for Ca^{II} since the former cause significant changes in chemical shifts and/or relaxation rates, and NMR results can therefore be analyzed for information on the structure of the complex. Throughout this paper, ligands and their complexes are expressed in terms of the number of oxidized saccharide units contributed; *i.e.* in $Dy(DCN)_2$, the ligand DCN contributes two oxidized saccharide units (two dicarboxy moieties) in order to complete the coordination sphere of Dy^{III} in the presence of water.

Dy^{III}-Induced ^{17}O Shifts. In order to derive information on oxygen complexation sites present in the ligand molecules, a series of Dy^{III}-induced ^{17}O shift NMR experiments was carried out. In order to ensure that the exchange between bound and bulk water is rapid, the experiments were carried out at 71 °C and 27.12 MHz. Addition of a Dy^{III} salt to an aqueous ligand solution results in a shift of the water ^{17}O signal to a lower frequency as a linear function of the molar ratio of Dy^{III} to ligand (ρ_L), which indicates that the condition of rapid exchange is fulfilled. This was further confirmed by experiments at room temperature and 54.31 MHz, which yielded similar results.[11] The observed Dy^{III}-induced shift thus represents an average of the chemical shifts of bound and free water molecules. We have previously shown that the Dy^{III}-induced shifts of ^{17}O nuclei coordinated to Dy^{III} are predominantly of contact origin and that the magnitude of these shifts always lies in a narrow range irrespective of other ligands coordinated to the Ln^{III} ion.[12] A plot of the net induced ^{17}O shift of water as a function of ρ_L (ρ_L = mol Dy^{III}/mol DCF), Figure 1, exhibits a change in gradient at $\rho_L = 0.5$ corresponding to a change in complex stoichiometry from $Dy(DCF)_2$ to Dy(DCF). If the same data are plotted against ρ_w, (mol of Dy^{III}/mol of D_2O), the slopes of the graphs are proportional to the number of water molecules binding to Dy^{III} (N_W). In the absence of organic ligand, the gradient is −18 778 ppm and since under these conditions $N_W = 8$, each bound water molecule can be associated with a shift of −2347 ppm. The hydration numbers found are 1.8 ± 0.5 for $Dy(DCF)_2$, (−4126/−2347), and 5.0 ± 0.5 for Dy(DCF), (−11988/−2347). Since the most common coordination number of Ln^{III} complexes of this type is 9, the data imply that there are three to four DCF donor sites in $Dy(DCF)_2$ and four DCF donor sites in the Dy(DCF) complex. Dicarboxylate compounds with bridging ethereal oxygen atoms are well-known as good chelators of Ca^{II}, usually binding tridentately to the metal cation. The oxydiacetate ligand (ODA) (Figure 2) has been previously

(5) (a) Peters, J. A.; Huskens, J.; Raber, D. J. *Prog. Nucl. Magn. Reson. Spectrosc.* **1996**, *28*, 283. (b) Sherry, A. D.; Geraldes, C. F. G. C. In *Lanthanide Probes in Life, Chemical and Earth Sciences*; Bünzli, J.-C. G., Choppin, G. R., Eds.; Elsevier: Amsterdam, 1989; Chapter 4. (c) Shannon, R. P. *Acta Crystallogr.* **1976**, *A32*, 751.
(6) Choppin, G. R. In *Lanthanide Probes in Life, Chemical and Earth Sciences*; Bünzli, J.-C. G., Choppin, G. R., Eds.; Elsevier: Amsterdam, 1989; Chapter 1.
(7) Johnson, L.; Verraest, D. L.; van Haveren, J.; Hakala, K.; Peters, J. A.; van Bekkum, H. *Tetrahedron Asymmetry* **1994**, *5*, 2475.
(8) Besemer, A. C. Publication in preparation.
(9) Levy, G. C.; Peat, I. R. *J. Magn. Reson.* **1975**, *18*, 500.
(10) (a) Haasnoot, C. A. G.; de Leeuw, F. A. A. M.; Altona, C. *Tetrahedron* **1980**, *36*, 2783. (b) Haasnoot, C. A. G.; de Leeuw, F. A. A. M.; Altona, C. *Org. Magn. Reson.* **1981**, *15*, 43. (c) Cerda-García, C. M.; Zepeda, L. G.; Joseph-Nathan, P. *Tetrahedron Comput. Methodol.* **1990**, *3*, 113.
(11) (a) Besemer, A. C.; van Bekkum, H. *Starch* **1994**, *46*, 419. (b) Besemer, A. C. Ph.D. Thesis, Delft University of Technology, 1993.
(12) Alpoim, M. C.; Urbano, A. M.; Geraldes, C. F. G. C.; Peters, J. A. *J. Chem. Soc., Dalton Trans.* **1992**, 463, and references therein.

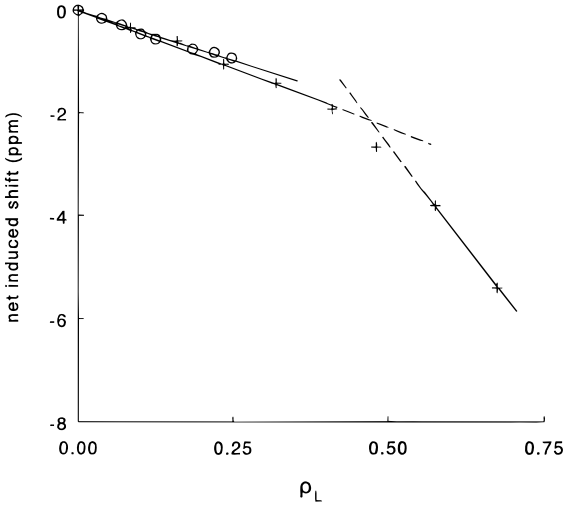

Figure 1. Net Dy^{III}-induced ^{17}O shift of water as a function of ρ_L for ligands DCF (+) and DCI (○).

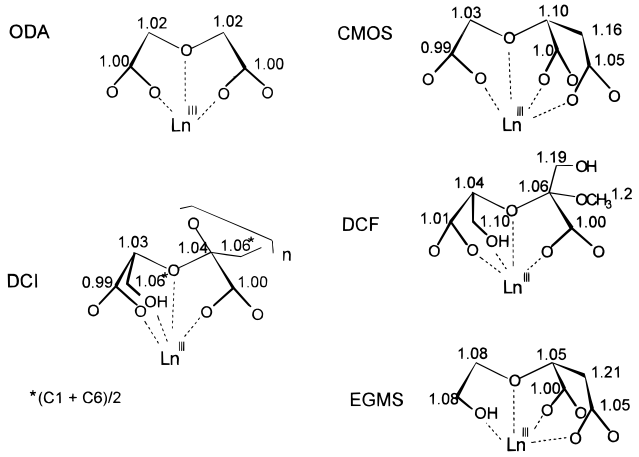

Figure 2. Ln^{III} complexes of DCF, DCI and similar ligands ODA, CMOS, and EGMS with relative $^{13}C-Gd^{III}$ distance ratios.

shown to bind tridentately to Ln^{III} and Ca^{II} ions.[13a,b,c] Thus a minimum of three donor sites is to be expected in the structurally similar DCF ligand. Binding by a fourth DCF donor site could be explained by interaction of hydroxyl functional groups with Dy^{III}.

Similar ^{17}O shift experiments were carried out with the ligands DCN and DCI. The hydration numbers found were 1.9 ± 0.5 for the $Dy(DCN)_2$ complex and 1.5 ± 0.5 for the $Dy(DCI)_2$ complex. Formation of a precipitate after $\rho_L = 0.25$ (ρ_L = molar ratio of Dy^{III} to oxidized saccharide units) prevented investigation of the Dy(DCN) and Dy(DCI) complex species using ^{17}O NMR techniques. DCN and DCI exhibit similar complexation behavior to DCF, with respect to $Dy(Ligand)_2$ complex formation (three to four ligand donor sites). The complexation behavior of similar ligands with Ca^{II} and Ln^{III}, disodium oxydiacetate (ODA), (carboxymethoxy)succinate (CMOS),[13] and ethylene glycol monosuccinate (EGMS),[14] has been previously investigated (Figure 2). ODA forms a 3:1 Ln^{III} complex containing no bound water molecules because nine ligand atoms complete the metal coordination sphere. The metal cation, the carbon and oxygen atoms of ODA all lie in one plane. The

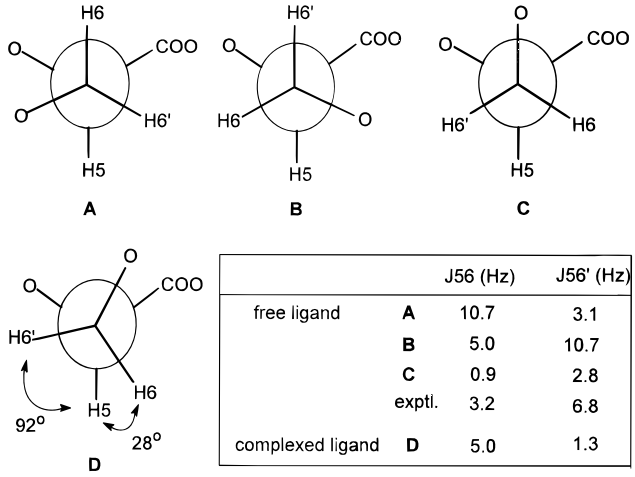

		J56 (Hz)	J56' (Hz)
free ligand	A	10.7	3.1
	B	5.0	10.7
	C	0.9	2.8
	exptl.	3.2	6.8
complexed ligand	D	5.0	1.3

Figure 3. Conformations and vicinal coupling constants, $^3J_{56}$ and $^3J_{56'}$ in free DCF (A−C) and in $La(DCF)_2$ (D).

CMOS ligand forms a $Dy(CMOS)_2(H_2O)$ complex composed of tetradentately and tridentately bound species existing in a dynamic equilibrium. EGMS forms a $Dy(EGMS)_2(H_2O)$ complex, and the ligand exhibits predominantly tetradentate behavior. These ligands bind in a similar manner as proposed for the DCF ligand, with a functional group, such as a hydroxyl or carboxylate moiety able to act as the fourth donor site of the ligand. Thus equilibria of tridentate and tetradentate binding modes are common for these type of ligands, and this is in agreement with the coordination behavior observed for DCF, DCN, and DCI.

Vicinal $^1H-^1H$ Coupling Constants ($^3J_{56}$ and $^3J_{56'}$) in the La^{III} Complexes. Since the ^{17}O NMR results had indicated tetradentate coordination by the DCF ligand, further evidence for interaction by a fourth donor site was sought. This was accomplished by investigating the behavior of the vicinal proton-proton systems of the C6 methylene protons, (H6 and H6′), and the C5 proton, (H5). The coupling constants $^3J_{56}$ and $^3J_{56'}$ as well as the chemical shifts of H5, H6 and H6′, were measured as a function of the diamagnetic La^{III} complex formation. In order to obtain estimates of $^3J_{56}$ and $^3J_{56'}$ in the free DCF ligand, three staggered rotamers may be taken into consideration, (Figure 3A−C), and coupling constant values can be estimated using an empirically generalized Karplus relationship.[10] Experimentally-derived values for the free DCF ligand are 3.2 Hz for $^3J_{56}$ and 6.8 Hz for $^3J_{56'}$, indicating rotamer B to be the most populated.

Addition of La^{III} to an aqueous DCF solution, causes $^3J_{56}$ to increase and $^3J_{56'}$ to decrease. The vicinal couplings in $La(DCF)_2$ can be resolved up to $\rho_L = 0.25$, after which point further coupling constant interpretation is prevented by merging of the vicinal proton signals. Extrapolation of a graph of ^3J vs ρ_L to $\rho_L = 0.5$ allows for estimation of values of $^3J_{56'} = 1.3$ Hz and $^3J_{56} = 5.0$ Hz for the $Dy(DCF)_2$ complex. Estimated ^3J values for the complexation of DCF suggest that a distorted conformation of rotamer C (Rotamer D, Figure 3) is predominant. A significant population of rotamers of type A and B would have been reflected in a higher value for $^3J_{56'}$. From the coupling constants, the dihedral angles between H5 and H6 and H6′ may be estimated to be 92 and 28°, respectively. The high preference for this conformation, indicates that the majority of the *C6*-hydroxyl groups participates in La^{III} coordination.

A similar change in vicinal coupling constants has been previously observed for the complexation of La^{III} by EGMS. In this case, the coupling constant values of the vicinal fragment change from 2.9 ($^3J_{23}$) and 10.9 Hz ($^3J_{23'}$) in the free ligand, to

(13) (a) Vijverberg, C. A. M.; Peters, J. A.; Bovée, W. M. M. J.; Kieboom, A. P. G.; van Bekkum, H. *Recl. Trav. Chim. Pays-Bas* **1983**, *102*, 255. (b) Uchtman, V. A.; Oertel, R. P. *J. Am. Chem. Soc.* **1973**, *95*, 1802. (c) Albertsson, J. *Acta Chem. Scand.* **1968**, *22*, 1563.
(14) Zhi, C.; van Westrenen, J.; van Bekkum, H.; Peters, J. A. *Inorg. Chem.* **1990**, *29*, 5025.

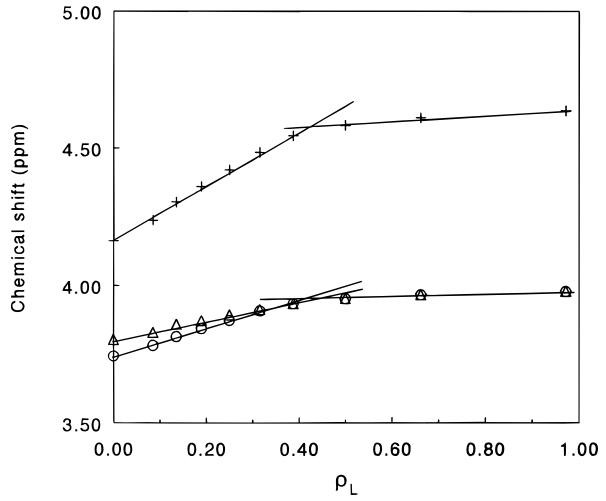

Figure 4. Chemical shifts of H6 (△), H6′ (○) and H5 (+) as a function of ρ_L (ρ_L = mol of La^{III}/mol of DCF).

5.4 ($^3J_{23}$) and 1.2 Hz ($^3J_{23'}$) in the Ln(EGMS) complex. The accompanying conformational changes are interpreted by associating the corresponding dihedral angles with a synclinal configuration of the carboxylate groups and the hydroxyl group. Thus the rearrangement effectively allowed for interaction by the fourth site (a carboxylate group attached to a methylene carbon atom, Figure 2). Tetradentate coordination by CMOS exhibits similar changes in vicinal coupling constants with the fourth site also adopting a synclinal conformation with respect to the other oxygen binding sites in the vicinal fragment.[10a,12,13]

The ^{17}O NMR experiments on $Dy(DCF)_2$ complexes reflected a mixture of tri- and tetradentate interaction. The equilibrium tetradentate ⇄ tridentate interaction probably shifts to the right hand side for Dy^{III} complexes, (Dy^{III} ionic radius: 1.08 Å (CN = 9)[5c]), due to an increase in steric crowding and concomitant decrease in proportion of tetradentate binding in comparison to La^{III} complex formation (La^{III} ionic radius: 1.22 Å (CN = 9)[5c]). A similar experiment was carried out with Lu^{III} (ionic radius: 1.03 Å (CN = 9)[5c]) in order to determine the effect of ionic radius on coupling constants.[5] Adding Lu^{III} to an aqueous DCF solution results unfortunately in the immediate merging of proton signals thus preventing resolution of ^3J coupling constant values. Comparison of the chemical shift changes of H5, H6, and H6′, as a function of ρ_L for both La^{III} and Lu^{III}, revealed the greatest change for H5 with a change in slope occurring at $\rho_L = 0.5$. This may be associated with the formation of Ln(DCF) at this point. Figure 4 shows the change in chemical shift as a function of ρ_L for La^{III} complex formation.

Lanthanide-induced shifts arise from the contributions by diamagnetic, contact, and pseudocontact effects occurring in Ln^{III} complexes. The diamagnetic contribution has been shown to be small using La^{III} and Lu^{III}. From theory it is known that paramagnetic lanthanides are able to induce shifts to lower frequencies or to higher frequencies via contact and pseudocontact mechanisms.[5] Complexes of sodium glycolate and ODA with Pr^{III} (1.18 Å (CN = 9)[5c]) and Yb^{III} (1.04 Å (CN = 9)[5c]) experienced ^1H proton shifts in a positive and negative direction respectively.[5,15] This trend was however not found in the case of DCF for $\rho_L < 0.5$, in addition to which, H6, H6′, and H5 exhibited the same direction of shift change contrary to predictions by theory. Furthermore, the ratio of the Pr^{III}:Yb^{III} induced shifts of the DCF methyl protons (C7) ($\rho_L < 0.5$) is much larger than that predicted by theory.[16] Thus considerable conformational changes take place across the Ln^{III} series for DCF complexation.

Table 1. Gradients ($1/(T_{1,M} + \tau_M)$) of Graphs of $1/T_{1,obs}$ as a Function of ρ_L for ^{13}C Nuclei in $Gd(DCF)_2$ and $Gd(DCI)_2$ Complexes (T = 298 K, [Gd^{III}] < 10^{-3}M, [ligand] = 0.5 M)

	DCF ($\times 10^3$)	DCI ($\times 10^3$)
C3	8.31	0.79
C4	7.71	0.70
C5	6.75	0.68
C2	6.01	0.61
C6	4.67	0.55[a]
C1	2.88	
C7	2.26	

[a] The signals for C1 and C6 coincide.

Gd^{III}-Induced Relaxation Rate Enhancements. The enhancement of longitudinal ($1/T_1$) relaxation rates of nuclei in ligands coordinating to Ln^{III} cations, is a phenomenon which enables an investigation of the environments experienced by these nuclei. Of all the lanthanides, Gd^{III} possesses the largest enhancement effect because it has a relatively long longitudinal electron spin relaxation time. Longitudinal relaxation rates of ^{13}C ligand nuclei in a Gd^{III} complex undergo enhancement by relaxation via dipolar interaction between the spins of the unpaired electrons in the Gd^{III} cation and the nuclear spins of the ligand atoms. Gd^{III} exerts a strong relaxation effect, thus nuclei in binding ligands experience a considerable shortening of their relaxation times, in addition to which, the use of low Gd^{III} concentrations ($\rho < 10^{-3}$) means that the complex species containing the maximum number of coordinated ligand is formed, *i.e.* $Gd(DCF)_2$. The relaxation rates of nuclei in the bound ligand, $1/T_{1,M}$ are related to the experimental values, $1/T_{1,obs}$ via eq 1, irrespective of the exchange regime between

$$\frac{1}{T_{1,obs}} = \frac{n\rho_L}{T_{1,M}+\tau_M} + \frac{1}{T_{1,free}} \qquad (1)$$

bound and free ligand nuclei.[17] $1/T_{1,free}$ is the relaxation rate of ^{13}C nuclei in the unbound ligand, τ_M is the residence lifetime of the complex, and n is the number of ligands participating in binding, ($n = 2$ in the present case). In accordance with eq 1, plots of $1/T_{1,obs}$ (at 25 °C) vs ρ_L yielded straight lines for each ligand ^{13}C nucleus (correlation coefficients >0.98) with gradients of $2/(T_{1,M} + \tau_M)$. The relaxation rate data for $Gd(DCF)_2$ and $Gd(DCI)_2$ are presented in Table 1.

For relatively weak ligands, such as DCF, $T_{1,M} \gg \tau_M$, so that the contribution of τ_M to the gradients of the plots of $1/T_{1,obs}$ vs ρ_L is negligible. $1/T_{1,M}$ is related to the molecular structure via eq 2, the simplified Solomon-Bloembergen equation,[18] in

$$\frac{1}{T_{1,M}} = \frac{2}{5}\left(\frac{\mu_0}{4\pi}\right)^2 \frac{\gamma_I^2 \mu_{eff}^2 \beta^2}{r^6} \tau_R \qquad (2)$$

which r represents the distance between Gd^{III} and a coordinated ^{13}C nucleus, τ_R is the rotational correlation time of the complex, ($\mu_0/4\pi$) is the magnetic permeability in a vacuum, γ_I is the magnetogyric ratio of the ^{13}C nucleus, μ_{eff} is the effective magnetic moment of the Gd^{III} ion, and β is the Bohr magneton.

For small molecules at the extreme narrowing limit, the τ_R values can be estimated from the dipole-dipole relaxation rates

(15) Peters, J. A.; Nieuwenhuizen, M. S.; Kieboom, A. P. G.; Raber, D. J. *J. Chem. Soc., Dalton Trans.* **1988**, 723.

(16) Bleaney, B. *J. Magn. Reson.* **1972**, *8*, 91.

(17) (a) Leigh, J. S., Jr. *J. Magn. Reson.* **1971**, *4*, 308. (b) McLaughlin, A. M.; Leigh, J. S., Jr. *J. Magn. Reson.* **1973**, *9*, 296. (c) Swift, T. J.; Connick, R. E. *J. Chem. Phys.* **1962**, *37*, 307.

(18) (a) Solomon, I. *Phys. Rev.* **1955**, *99*, 559. (b) Bloembergen, N. *J. Chem. Phys.* **1957**, *27*, 572.

Table 2. Nuclear Overhauser Enhancements (η_{obs}) and Longitudinal Relaxation Rates ($1/T_{1,obs}$) for the Determination of Rotational Correlation Times (τ_R) for $La(DCF)_2$

^{13}C nucleus	η_{obs}[a]	$1/T_{1,obs}$ (s^{-1})	$1/T_{1,DD}$ (s^{-1})	τ_R (s)
C5	1.17	3.04	1.78	9.2×10^{-11}
C6	1.53	4.85	3.71	9.6×10^{-11}
C1	1.46	5.03	3.67	9.5×10^{-11}
C7	1.04	0.91	0.47	8.1×10^{-12} [b]

[a] Evaluated from measurements at $\rho_L = 0$ and $\rho_L = 0.24$. [b] Omitted in the calculation of an average τ_R value, $\tau_R = 9.4 \times 10^{-11}$ s.

Table 3. Interatomic ($Gd^{III}-^{13}C$) Distances, Experimental and Estimated from Molecular Models for $Gd(DCF)_2$

DCF	*r*(exptl) (Å)	*r*(estimated) (Å)
C3	3.24	3.20
C4	3.28	3.20
C2	3.42	3.39
C5	3.34	3.39
C1	3.87	4.00
C6	3.57	3.80
C7	4.03	4.50

($1/T_{1,DD}$) of the ^{13}C nuclei in the corresponding diamagnetic La^{III} complex (eq 3). Here, *N* represents the number of protons

$$\frac{1}{T_{1,DD}} = N\left(\frac{\mu_0}{4\pi}\right)^2 \frac{\hbar^2\gamma^2[^{13}C]\gamma^2[^1H]}{r_{CH}^{\ 6}}\tau_R \qquad (3)$$

bound to the ^{13}C nucleus, r_{CH} the bond length between a proton and a ^{13}C nucleus, $\hbar$ the Dirac constant, and $\gamma[^{13}C]$ and $\gamma[^1H]$ the magnetogyric ratios of the ^{13}C and ^1H nuclei, respectively.

The dipole−dipole contribution to the observed relaxation rate ($1/T_{1,obs}$) was estimated using eq 4, in which η_{obs} is the

$$\frac{1}{T_{1,DD}} = \frac{\eta_{obs}}{1.988T_{1,obs}} \qquad (4)$$

nuclear Overhauser enhancement (see Table 2). With this procedure, a τ_R value of 9.4×10^{-11} was obtained for DCF at 25 °C.

The Debye−Stokes−Einstein equation (eq 5) relates τ_R to the volume of the complex with the assumption that the species concerned are spherical.[19] Here *a* represents the complex radius,

$$\tau_R = \frac{4\pi a^3\eta}{3kT} \qquad (5)$$

η the viscosity, *k* the Boltzmann constant, and *T* the temperature. Using an estimated complex radius $a = 4$ Å and assuming the viscosity to be equivalent to that of water (2×10^{-3} Pa s), a τ_R value of 1×10^{-10} s was calculated. This is close in value to the τ_R value derived from the NMR experiments.

$^{13}C-Gd^{III}$ distances were obtained using eq 2 and were compared with values estimated from computer and Dreiding models of the $Gd(DCF)_2$ complex in which tetradentate interaction was assumed (Table 3). As the experimental values correspond well with the estimated values, the neglect of τ_M is justified. The relatively shorter $Gd^{III}-^{13}C$ distances of carboxylate carbon atoms C3 and C4 evidence the binding of the carboxylate oxygen atoms to the Gd^{III} ion. The NMR results locate the C6 atom of DCF 3.57 Å away from the Gd^{III} atom. From molecular models, it may be estimated that in the case of no interaction by the C6 hydroxyl moiety, the backbone of the oxidized saccharide unit would be approximately planar and a $C6-Gd^{III}$ distance of approximately 4 Å would be expected.

Table 4. Nuclear Overhauser Enhancements (η_{obs}) and Longitudinal Relaxation Rates ($1/T_{1,obs}$) for DCI

^{13}C nucleus	η_{obs}	$1/T_{1,obs}$ (s^{-1})
C5	0.55	4.55
C1 + C6[a]	0.56	7.14

[a] The signals for C1 and C6 coincide.

For DCI, the rotational correlation time (τ_R) is expected to be higher than for DCF due to the polymeric character of the molecule. Therefore, higher values for the gradients $1/T_{1,M}$ are expected, which is in contrast with the experimental results (Table 1). This phenomenon might be explained by a higher value of residence time of Gd^{III} in the complex (τ_M), which contributes significantly to the gradients of $1/T_{1,obs}$ versus ρ_L (see eq 1).

For these high molecular weight compounds, the extreme narrowing limit does not apply. This is reflected in the very low nuclear Overhauser effect measured for ^{13}C in the free ligand (DCI) (Table 4). From a comparison of the observed nuclear Overhauser effect and the T_1 values to plots of T_1 and NOE as a function of the rotational correlation time, constructed with the use of the procedure described by Howarth[20] and Huckerby,[21] τ_R was estimated to be 1.6×10^{-9} s. We assume that the Ln^{III} complexes of DCI have about the same molecular volume as the free ligand and, therefore, about the same τ_R value. The value obtained is in agreement with what would be expected based on the higher molecular volume (eq 5) and with the reported value for dextran (average DP = 100), $\tau_R = 1.4 \times 10^{-9}$ s at 60 °C.[21] Using this value for τ_R and the known $^{13}C-Gd^{III}$ distance of the carboxylates (C3, C4) of DCI (3.2 Å, cf. value found for DCF), $T_{1,M}$ can be calculated via eq 2. The value for τ_M was then calculated via eq 1 and was found to be 1.34×10^{-3} s. This value is in agreement with the τ_M found for ligands with comparable binding strengths for Ln^{III}, such as triphosphate ($\tau_M = 2 \times 10^{-3}$ s at 25 °C).[22]

In order to compare the binding of ligands DCF, DCI, ODA, CMOS, and EGMS, it is useful to examine their relative $^{13}C-Gd^{III}$ distance ratios. These may be calculated from the sixth root ratio of relative relaxation rate enhancements of ^{13}C nuclei, *i.e.* $1/T_{1,M}$ of a nucleus i relative to a nucleus j in the same ligand. The distance ratio values were calculated relative to a carboxylate ^{13}C nucleus in each ligand and are presented in Figure 2. All ^{13}C nuclei directly bonded to coordinating oxygen atoms (carboxylates and etherial oxygen for tridentate coordination) possess short relative distance ratios (≤1.10). For ligands exhibiting tetradentate behavior (DCF, CMOS and EGMS), the ^{13}C nucleus directly bonded to the fourth binding site also possesses a short relative distance ratio. Molecular models indicate that the otherwise planar oxidized saccharide unit of the DCF ligand probably undergoes distortion in order to achieve tetradentate coordination as has been previously found for CMOS.[10a]

Similar trends were observed in the case of the DCI ligand, although the results have to be handled with caution. First, the ^{13}C NMR signals of the primary alcohol groups (C1 and C6) coincide. The observed longitudinal relaxation rates are thus an average of both C atoms. It is likely that the distance of

(19) (a) Reuben, J. *J. Phys. Chem.* **1975**, *79*, 2154. (b) Bloembergen, W.; Purcell, E. M.; Pound, R. V. *Phys. Rev.* **1948**, *73*, 679.

(20) Howarth, O. In *Multinuclear NMR*; Mason, J., Ed.; Plenum Press: London, 1987; Chapter 5.

(21) Huckerby, T. N.; Nieduszynski, I. A. *Int. J. Biol. Macromol.* **1982**, *4*, 269.

(22) Nieuwenhuizen, M. S.; Peters, J. A.; Sinnema, A.; Kieboom, A. P. G.; van Bekkum, H. *J. Am. Chem. Soc.* **1985**, *107*, 12.

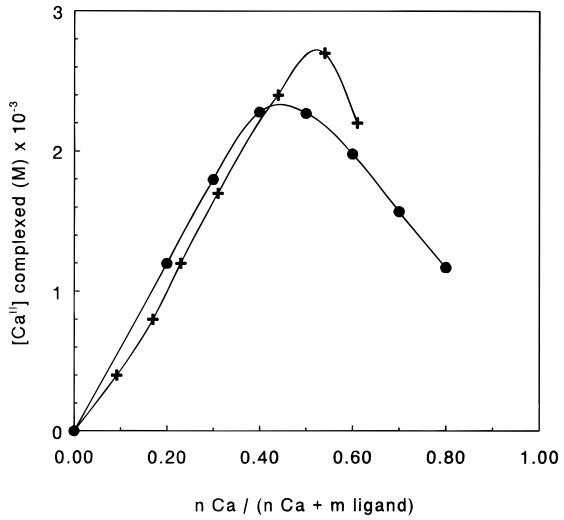

Figure 5. Job's plot of [Ca−complex] as a function of *n*Ca/(*n*Ca + *m* oxidized saccharide units), for ligands DCI (●) and DCN (+). [*n*Ca + *m* oxidized saccharide units] = 6 mM. The curves are guides to the eye.

C6−Gd^{III} is shorter than the distance of C1−Gd^{III} (tetradentate binding involving C6), but this could not be verified by these experiments. Second, the observed longitudinal relaxation rate enhancements are determined not only by $1/T_{1,M}$ but also by $1/\tau_M$ (see above).

Coordination with Ca^{II}. Complexation studies were carried out with Ca^{II} since the nature and extent to which binding occurs are of relevance with respect to the Ca^{II} sequestering applications of the ligands concerned.

In order to verify that the stoichiometries of the Ln^{III} and Ca^{II} complexes are comparable, vicinal coupling constants and chemical shifts of the C6 methylene protons, (H6, H6′) of DCF were monitored as a function of ρ_L, (ρ_L = mol Ca^{II}/mol DCF). The vicinal signals merge after $\rho_L = 0.28$, at which point $^3J_{56}$ has increased to 3.7 Hz and $^3J_{56'}$ has decreased to 4.8 Hz. These changes are comparable though smaller than those found in the La^{III} complexation. The H5 proton exhibited the greatest change with respect to chemical shift. Thus it can be deduced that the conformational changes taking place during Ca^{II} complex formation are comparable with those occurring during Ln^{III} complexation. The ligand CMOS has also been found to exhibit comparable coupling constant and chemical shift changes during complexation with Ln^{III} and Ca^{II}.[10a]

Predominance of a 1:2 complex species, *i.e.* Dy(DCN)$_2$ and Dy(DCI)$_2$, at $\rho_L < 0.25$, has been shown from the results of ^{17}O NMR experiments. Precipitate formation at $\rho_L > 0.25$ prevented further measurement; thus investigation for the occurrence of the 1:1 complexes, Dy(DCN) and Dy(DCI), using NMR methods was not possible. The latter type of complexes were therefore studied with Ca^{II} as the metal ion using potentiometry because the dilute conditions employed (6 mM ligand solution) did not result in precipitation.

The stoichiometry of the Ca-DCI complexes at high ρ_L values was determined via a so-called Job's plot (Figure 5). A Job's plot expresses the complex concentration (equivalent to the concentration of bound Ca^{II}) as a function of *n*Ca/(*n*Ca + *m*ligand), in which (*n*Ca + *m*ligand) is kept constant (*n*Ca = mol of Ca^{II}, *m*ligand = equiv of oxidized saccharide units). A maximum in the plot is found when the complex with the highest Ca:ligand ratio is formed. Job's plots were constructed by mixing Ca^{II} and ligand solutions in various ratios *n*Ca/(*n*Ca + *m*ligand) so that the total concentration (*n*Ca + *m*ligand) was 6 mM. The complex concentration was measured by measuring the concentration of uncomplexed Ca^{II}, using a Ca^{II} ion-selective electrode. The Job's plots of DCI and DCN exhibit maxima at *n*Ca/(*n*Ca + *m*ligand) ≈ 0.5, confirming the presence of 1:1 complexes at higher ρ_L values.[23] A comparison of the shape and position of the maximum of these Job's plots with those simulated for various values of stepwise stability constants, K_1 and K_2, indicates that the stabilities of the 1:1 and 1:2 complexes are of the same magnitude. Since the results of NMR experiments on DCI at $\rho_L < 0.5$ had indicated the presence of 1:2 complexes, the change in complex stoichiometry at ρ_L = 0.5 is assumed to occur like in the case of DCF, in which the complex stoichiometry had been determined completely with NMR experiments.

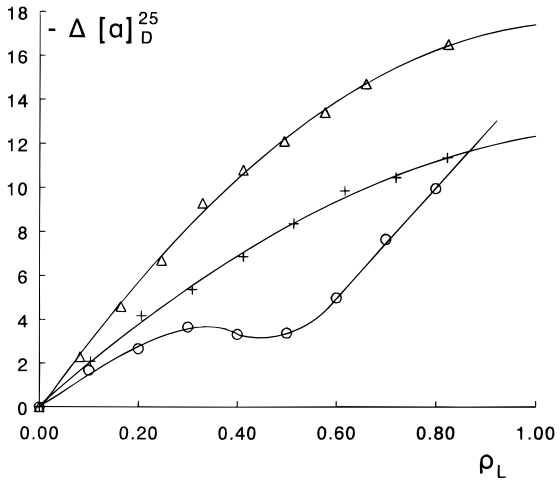

Figure 6. Change in optical rotation as a function of ρ_L (ρ_L = mol Ca^{II}/mol oxidized saccharide unit), for ligands DCF (+), DCN (△) and DCI (○). The curves are guides to the eye.

The conformational changes occurring in ligands during Ca^{II} complexation were also monitored by optical rotation measurements. The optical rotation of ligand solutions containing appropriate amounts of Ca^{II} were measured. Figure 6 shows the change in optical rotation with respect to that of the free ligand, $\Delta[\alpha]_D^{25}$, as a function of ρ_L. Optical rotation values for the complexation of DCF and DCN with Ca^{II} decrease with increasing Ca^{II} concentration, which points to a gradual change in conformation going from free ligand to complexed ligand. For DCI, a completely different behavior was observed. There, the curve of $-\Delta[\alpha]_D^{25}$ versus ρ_L showed a local maximum at ρ_L = 0.3 and a local minimum at $\rho_L = 0.5$. However, the NMR studies did not suggest any change of the coordination of the metal ion at $\rho_L = 0.3$; up to $\rho_L = 0.5$, the metal ion is coordinated by two oxidized fructose units. Most likely, this coordination is intramolecular, as shown by viscosity measurements (see below), so torsion of the DCI backbone and folding is required to coordinate the metal ions. At $\rho_L = 0.3$, two out of three oxidized fructose units are bound to a metal ion. Apparently, an increase of ρ_L brings about a drastic conformational change, probably due to a transition between a loosely folded chain to a more extensively folded one. Obviously, another transition occurs at $\rho_L = 0.5$, since then 1:1 complexes are formed, as indicated by the Job's plot. This phenomenon was not observed for DCN, probably because this molecule is too short (four saccharide units) to experience intensive folding.

The Ca^{II} sequestering capacities (SC) of DCF, DCN, and DCI were determined since the strength of Ca^{II}-binding by the oxidized saccharide systems is of relevance to sequestration applications. In these experiments, a solution of 100 mg of

(23) Gil, V. M. S.; Olivera, N. C. *J. Chem. Educ.* **1990**, *67*, 473.

ligand in 100 mL of water, (ionic strength = 0.02 M, NaCl, pH = 10.2, NH_3), was titrated with a Ca^{II} solution (0.1 M), the course of the complexation being followed by measuring the concentration of uncomplexed Ca^{II} present using a Ca^{II} ion-selective electrode. The sequestering capacity (SC) is defined as the mmol of Ca^{II} that can be added to 1 g of ligand until the concentration of noncomplexed $Ca^{II} = 10^{-5}$ M. SC values obtained are reported in units of millimoles of Ca^{II} bound per gram of ligand: DCF = 0.76; DCN = 1.3, and DCI = 2.1. DCF possesses thus a reasonably small SC whereas that of DCN is moderately high. The SC value obtained for DCI is very high and makes the material applicable as sequestering agent.[11]

According to the theory of multiple equilibria for polyelectrolytes in which identical electrostatically interacting complexing sites are involved, the stability constants of the complex (K) can be determined using eq 6a in which Z is the fraction of

$$K = \frac{Z}{(1 - Z)[\mathrm{Ca}]} = K_{\mathrm{intr}} e^{cZ} \qquad (6a)$$

sites occupied by Ca^{II} ions.[24,25] The intrinsic stability constant (K_{intr}) is defined as the value of K at $Z = 0$, and can be determined by plotting the data, obtained by the titration experiments described above, according to the logarithmic form of this equation (Tanford plot) (eq 6b, $a = c \log(e)$). The

$$pCa^{II} + \log \frac{Z}{1 - Z} = aZ + \log K_{\mathrm{intr}} \qquad (6b)$$

concentration of ligand was calculated as the concentration of oxidized monosaccharide units. Calculation of Z was based on a complex stoichiometry of 1:1 as was indicated by the Job's plots. In this eq 6a, c is a constant which depends on the electrostatical free energy of a complexing site and the parameters determining this energy (radius, length, ionic strength, temperature).[24] According to the theory, linear plots were obtained for $\rho = 0.1-0.7$. Values of log K_{intr} of 4.5 (DCF), 6.4 (DCN), and 8.2 (DCI) were obtained. The log K was observed to decrease with increasing Ca^{II} association, due to a decreasing affinity of Ca^{II} for the polymer upon complexation because of the accompanying increase in mutual repulsion. This decrease in affinity is given by the slope of the Tanford plots: $a = -6.3$ for DCI and -5.3 for DCN, respectively. The ligands DCF and ODA did not exhibit any decrease since they are single complexing units and do not exhibit polyelectrolyte behavior. The log K value of ODA has been previously determined to be 3.9,[25] which is lower than the value determined for DCF, (log $K = 4.5$). DCF chelates more strongly because it has a fourth binding site.

In order to determine whether the course of binding of Ln^{III} ions to DCI is similar to Ca^{II} ions, a Tanford plot was constructed from the datapoints of a titration of 100 mg of ligand in 100 mL of water with a 0.1 M Pr^{III} solution. The concentration of uncomplexed Pr^{III} ions was followed during the titration using a Ca^{II} ion-selective electrode which was calibrated with $10^{-5}-10^{-2}$ M $PrCl_3$ solutions. Accurate electrode readings during titration were hindered due to the nonlinearity of the electrode at low Pr^{III} concentrations ($\rho_L < 0.4$) and precipitation of Pr^{III}–DCI complexes at $\rho_L > 0.6$. For these reasons, the Tanford plot obtained was not linear and determination of a K_{intr} was not possible. However, it was clear that

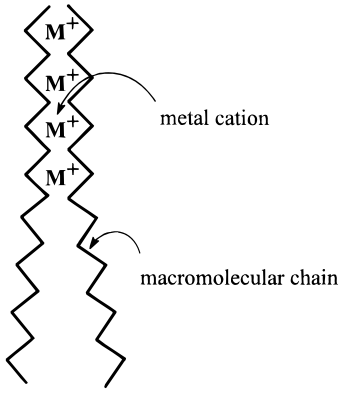

Figure 7. "Egg-box" model of macromolecular binding of metal cations.

log K decreased with increasing Pr^{III} association, pointing to a decreasing affinity upon complexation. These results confirm that lanthanide ions are good mimics of calcium.

The decreasing affinity of Ca^{II} (or Ln^{III}) for the oxidized polysaccharides, DCN and DCI, upon complexation indicates that the binding of Ca^{II} ions is anticooperative, in contrast to macromolecules which bind metal ions according to the "egg-box" model (Figure 7), in which an array of metal ions is held between macromolecular chains.[26] The firm binding of some divalent cations, *e.g.* Ca^{II}, on polyguluronate and pectate, and the high selectivity of these polyuronates in ion exchange reactions are mainly due to the intermolecular binding of metal cations according this model, in which two or more chains participate in cooperative coordination of the metal cation and an ordered tertiary structure is formed. The gelation of alginate upon chelation with Ca^{II} is explained by cooperative junction zone formation by interchain association in which Ca^{II} ions occupy interstices between parallel alginate chains.[23]

In the case of DCN and DCI, it is therefore most likely that the $Ca(DCN)_2$ complex is formed either by interaction between adjacent pairs of oxidized binding units or else by folding its backbone so that oxidized saccharide units opposite to each other form a coordination sphere. DCI is composed of oxidized saccharide units which are attached to a backbone. The oxidized saccharide units do not form part of the polymer backbone and are separated by three bonds; this results in a fairly loosely jointed polymer in which the binding entities, the oxidized saccharide units, are not subject to severe steric hindrance. DCI is therefore a polyelectrolyte with a relatively high degree of rotational freedom, and hence low rigidity, which would be unlikely to adopt a stable, regular helical conformation in solution at room temperature. Various theories concerning the conformation of unoxidized inulin (I) in solution exist, *i.e.* helical versus nonhelical, although none have conclusively proven the existence of a regular or a helical form.[27] As the Tanford data obtained for DCI do not reflect cooperative binding, the existence of a regular helical complex is unlikely. DCI is a relatively short chain polymer, which is experiencing thermal collisions at room temperature. Studies on the chain length dependence of polyguluronate upon Ca^{II}-binding activity showed that cooperative binding only takes place above a certain degree of polymerization, (DP > 20).[23]

Alginates have been observed to undergo gelation accompanied by a sharp increase in viscosity during their

(24) Tanford, C. *Physical Chemistry of Macromolecules*; Wiley: New York, 1961; pp 526–586.
(25) Floor, M.; Peters, J. A.; van Bekkum, H.; Kieboom, A. P. G.; Koek, J. H.; Smeets, F. L. M.; Niemantsverdriet, R. E. *Carbohydr. Res.* **1990**, *203*, 19.
(26) (a) Rees, D. A. *Polysaccharide Shapes*; Chapman and Hall: London, 1977. (b) Morris, E. R.; Rees, D. A.; Thom, D.; Boyd, J. *Carbohydr. Res.* **1978**, *66*, 145. (c) Kohn, R. *Pure Appl. Chem.* **1975**, *42*, 371.
(27) (a) Liu, J.; Waterhouse, A. L.; Chatterton, N. J. *J. Carbohydr. Chem.* **1994**, *13*, 859. (b) Oka, M.; Ota, N.; Mino, Y.; Iwashita, T.; Komura, H. *Chem. Pharm. Bull.* **1992**, *40*, 1203.

cooperative chelation of Ca^{II}. We therefore investigated for the occurrence of interchain binding in the complexation of Ca^{II} by DCI, by measuring viscosity as function of ρ_L (ρ_L = mol of Ca^{II}/mol of DCI). A negligible increase in viscosity attributable to the increase in Ca^{II} salt concentration was observed. Thus there is no evidence for an increase in viscosity indicative of cross-linking, *i.e*. the occurrence of interchain chelation is most unlikely.[24] This provides additional support for noncooperative Ca^{II} binding by DCI. The latter probably adopts a random coil chain configuration in which metal cation-binding takes place mainly via interaction between adjacent oxidized saccharide units. Torsion of the backbone and chain folding is possible, as was indicated by the optical rotation measurements, and there may be minor interaction by the backbone oxygen atom, although this is not likely to be a dominant feature of strong Ca^{II}-binding. Anticooperative binding is observed probably because chelation becomes less favorable as charge saturation occurs with increasing Ca^{II} coordination.

Conclusions

Dy^{III}-induced ^{17}O NMR experiments with DCF, DCN, and DCI provided data on the ligand oxygen donor sites suggesting the existence of a tri- ⇄ tetradentate equilibrium. Determination of interatomic $^{13}C-Gd^{III}$ distances in $Gd(DCF)_2$ complexes verified the proposed mode of binding as tetradentate via, two carboxylate oxygen atoms, an ethereal oxygen atom, and a hydroxyl group. Potentiometric experiments with Ca^{II} reflected the strong binding abilities of compounds containing oxidized fructose units, indicating that these entities, with respect to structure and charge, are particularly suitable for the chelation of Ca^{II} ions. The presence of a fourth binding site results in an even more efficient sequestration of Ca^{II}. Conformational changes occurring in DCI during Ca^{II} complexation were studied via optical rotation measurements. Between $\rho_L = 0.3$ and $\rho_L = 0.5$, a dramatic change in conformation was observed, which was ascribed to intensive folding of the inulin chains in order to form 2:1 ligand−Ca complexes. The cooperativity of binding by DCF, DCN, and DCI was investigated potentiometrically but no evidence was found for preorganized, cooperative binding of Ca^{II} cations. Thus DCI, a loosely-jointed polyelectrolyte, is unlikely to bind metal ions in solution via stable helical or "egg-box" structures.

Acknowledgment. We would like to extend thanks to Dr. Bart Reuvers of Akzo Nobel Corporate Research for assistance with the viscosity measurements. We are grateful to Coöperatie Sensus Food Ingredients and to Südzucker for donating the inulin and nystose respectively. This research received financial support from the Dutch Ministry of Agriculture, Nature Management, and Fisheries as part of its Special Program on Carbohydrate Oxidation.

IC960103B